Small-Volume Nuclear Magnetic Resonance Spectroscopy

Raluca M. Fratila and Aldrik H. Velders

MIRA Institute for Biomedical Engineering and Technical Medicine, Faculty of Science and Technology, University of Twente, 7500 AE Enschede, The Netherlands; email: r.m.fratila@tnw.utwente.nl, a.h.velders@utwente.nl

Annu. Rev. Anal. Chem. 2011. 4:227–49

First published online as a Review in Advance on March 8, 2011

The *Annual Review of Analytical Chemistry* is online at anchem.annualreviews.org

This article's doi: 10.1146/annurev-anchem-061010-114024

1936-1327/11/0719-0227$20.00

Keywords

microcoils, mass-limited samples, microfluidics, hyphenated analytical techniques

Abstract

Nuclear magnetic resonance (NMR) spectroscopy is one of the most information-rich analytical techniques available. However, it is also inherently insensitive, and this drawback precludes the application of NMR spectroscopy to mass- and volume-limited samples. We review a particular approach to increase the sensitivity of NMR experiments, namely the use of miniaturized coils. When the size of the coil is reduced, the sample volume can be brought down to the nanoliter range. We compare the main coil geometries (solenoidal, planar, and microslot/stripline) and discuss their applications to the analysis of mass-limited samples. We also provide an overview of the hyphenation of microcoil NMR spectroscopy to separation techniques and of the integration with lab-on-a-chip devices and microreactors.

1. INTRODUCTION

Nuclear magnetic resonance (NMR) spectroscopy is one of the most powerful analytical techniques available; it has applications in chemistry, biology, physics, medicine, and materials science. The wealth of information provided by NMR spectroscopy is unsurpassed by any other technique. It includes (bio)molecular structure elucidation; studies of binding kinetics, molecular dynamics, and surface chemistry; and diagnostic imaging in medicine, among others. NMR spectroscopy is just over 60 years old, yet it has advanced remarkably in that short lifetime. Solution-state, gel-state, and solid-state NMR spectroscopy, as well as magnetic resonance imaging (MRI), are now common research tools, and the gallery of available mono- and multidimensional, homonuclear, and heteronuclear experiments is continuously expanding. The scientific community has widely recognized the importance and the impact of NMR spectroscopy, as illustrated by several Nobel prizes awarded for breakthrough discoveries in different disciplines (e.g., Rabi in 1944 and Bloch & Purcell in 1952 for physics; Ernst in 1991 and Wütrich in 2002 for chemistry; and Lauterbur & Mansfield in 2003 for physiology and medicine). Unfortunately, NMR spectroscopy is also the least sensitive of the standard analytical tools (1). Thus, applying NMR methods to mass- and/or volume-limited samples (e.g., characterization and identification of new natural products, analysis of metabolites, high-throughput screening of large libraries of compounds from combinatorial chemistry, lab-on-a-chip processes) represents a major challenge. We review the main achievements in the implementation of NMR spectroscopy to the analysis of small-volume samples over the past two decades. First, we give an overview of the general approaches to increase the sensitivity of an NMR experiment. Second, we discuss the state of the art of the miniaturization of NMR probes for liquid-state NMR spectroscopy. Finally, we describe the hyphenation of small-volume NMR spectroscopy with other analytical and microseparation techniques, as well as its integration with lab-on-a-chip devices and microreactors.

Lab on a chip: a device that integrates one or several laboratory functions on a single chip with a size of only millimeters to a few square centimeters

Hyphenation: combination of two (or more) separation and/or spectroscopic techniques within one analytical setup

B_0: static magnetic field about whose direction the nuclear magnetic moment precesses; usually expressed in tesla or as the Larmor proton precession frequency (e.g., 9.4 T or 400 MHz, respectively)

Signal-to-noise ratio (SNR): ratio between peak signal intensity and the root-mean-square noise level

B_1: the magnetic field generated by the RF coil (expressed in tesla)

2. STRATEGIES TO ENHANCE THE SENSITIVITY OF NUCLEAR MAGNETIC RESONANCE SPECTROSCOPY

Nuclei with nonzero spin interact with an external magnetic field (i.e., in a Zeeman interaction) (2) to give rise to the NMR phenomenon. For a nucleus with a spin quantum number $I = 1/2$ (such as the hydrogen nucleus), two energy levels defined as α (lower-energy state) and β (higher-energy state) are generated. The NMR signal is proportional to the population difference between the high- and low-energy states (N_α and N_β) and is described by the Boltzmann equation

$$\frac{N_\beta}{N_\alpha} = \exp\left(-\frac{\Delta E}{kT}\right) = \exp\left(-\frac{\hbar\gamma B_0}{kT}\right), \quad (1)$$

where ΔE is the energy difference between the two energy levels, h is the Planck constant ($\hbar = h/2\pi$), γ is the gyromagnetic ratio of the nucleus, B_0 is the strength of the applied magnetic field, k is the Boltzmann constant, and T is the temperature. In practice, this population difference is extremely small (1 part in 10^4, even with the strongest magnetic fields available), which leads to a significant sensitivity problem for NMR spectroscopy with respect to other standard analytical techniques, such as ultraviolet (UV)-visible or infrared (IR) spectroscopy. The signal-to-noise ratio (SNR) for an NMR experiment can be defined as (3)

$$\frac{k_0\left(\frac{B_1}{i}\right)V_s N \gamma\hbar^2 I(I+1)\frac{\omega_0^2}{k_B T 3\sqrt{2}}}{F\sqrt{4kT\,\Delta f(R_{coil}+R_{sample})}}, \quad (2)$$

where k_0 is a scaling factor including the radio-frequency (RF) inhomogeneity in the B_1 magnetic field produced by the probe; B_1/i is the magnetic field generated per unit current; V_s is the sample

volume; N is the number of spins per unit volume; I is the spin quantum number; ω_0 is the Larmor precession frequency (where $\omega_0 = \gamma B_0$); F is the noise factor of the spectrometer; R_{coil} and R_{sample} are the coil and sample resistances, respectively; and Δf is the spectral bandwidth.

Several technical solutions to increase the sensitivity of NMR spectroscopy have been successfully applied over the past few decades. The classical approach is represented by the use of higher–magnetic field strengths to maximize ω_0. The development of superconducting magnets rendered the high-resolution NMR spectrometers widely available; the world's first 23.5-T magnet (corresponding to a proton Larmor precession frequency of 1 GHz) was installed in 2009 at the Centre de Résonance Magnétique Nucléaire à Très Hauts Champs in Lyon, France. However, the costs associated with the development and installation of higher-field spectrometers increase exponentially with the field strength, whereas the sensitivity improves by only a factor of two when moving, for example, from 600 to 900 MHz (4, 5). The implementation of cryogenic probes, in which the thermal noise of the coil is substantially reduced by cooling the receiver coil and the preamplifiers to ~20 K, provides sensitivity gains of a factor of four when compared with conventional NMR probes at the same magnetic field strength (6–8). The use of cryoprobes, however, places high demands on thermal insulation and cooling (because the room temperature sample is located very close to the cooled receiver coil), and the installation and maintenance of cryoprobes are not trivial and are rather expensive. Another promising way to boost NMR sensitivity is based on hyperpolarization techniques to increase the population difference of the Zeeman levels of the nuclear spins. Several hyperpolarization and polarization transfer strategies have been developed, including optical pumping of ^{129}Xe nuclei via SPINOE (spin polarization–induced nuclear Overhauser enhancement) (9–11), CIDNP (chemically induced dynamic nuclear polarization) (12–14), PHIP (parahydrogen-induced polarization) (15–17), and microwave-driven polarization transfer from unpaired electron spins to coupled nuclear spins via DNP (dynamic nuclear polarization) (18–21). Although significant enhancement in the sensitivity of NMR spectroscopy experiments has been achieved and DNP-NMR spectrometers are now commercially available, the field remains open to many developments, both theoretical and experimental. In a completely different approach, namely remote detection, the NMR encoding and detection steps are separated both temporally and spatially (22), which allows the independent optimization of each step. This technique has been successfully used to enhance the sensitivity of NMR spectroscopy and imaging experiments (23, 24), and it has proven to be particularly useful for microfluidic devices (25–29).

Yet another way to increase the NMR sensitivity of particularly mass-limited samples is the use of microcoil probes. On the basis of the principle of reciprocity described by Hoult & Richards (3), Webb and coworkers (30) demonstrated that for a constant length-to-diameter ratio, the sensitivity of an NMR coil is inversely proportional to its diameter. This means that when the detection coil is miniaturized, the sample volume can be brought down to the nanoliter regime. The conventional NMR sample consists of a 5-mm-diameter glass tube with a fill volume of ~600 μl, but micro-NMR probes with volumes in the low microliter range are now available (see Related Resources). Below, we provide an overview of the state of the art of microcoils whose detection volumes are in the submicroliter range; for applications of high-resolution commercial microcoil probes with volumes that are higher than 1 μl, we encourage the interested reader to explore the cited literature (1, 5, 31–35). We briefly mention some relevant solid-state NMR and MRI applications, but a detailed description falls outside the scope of this review. Instead, we focus on the practical solutions that miniaturized detection NMR coils offer for the analysis of small-volume samples, and less on theoretical and technical aspects; for information about these issues, we direct the reader to several relevant papers.

T: tesla, the SI unit for magnetic field strength

DNP: dynamic nuclear polarization

Microcoils: RF (NMR) coils whose detection volumes are in the submicroliter range

3. HIGH-RESOLUTION LIQUID-STATE NUCLEAR MAGNETIC RESONANCE SPECTROSCOPY FOR SUBMICROLITER-SAMPLE VOLUMES

Spectral resolution: instrumental-performance figure of merit that determines the peak separation that can still be distinguished; usually expressed as peak full width at half maximum height

Magnetic susceptibility: degree of magnetization of a material in response to applied magnetic field

Limit of detection (LOD): normalized mass ($nLOD_m$) or concentration ($nLOD_c$) of sample necessary to acquire a desired SNR for a specific peak and a given acquisition time

To characterize and compare the performance of NMR probes, investigators usually employ several parameters, such as spectral resolution, SNR, sensitivity, and limit of detection (36). However, the choice for one or another of these figures of merit and the way they are defined strongly depend on the individual situation; see the reviews by Lacey et al. (1) and Olson et al. (31) for more detailed discussion.

Spectral resolution, usually defined as the line's full width at half maximum (FWHM), represents a serious limitation in the use of microcoils because it is compromised by susceptibility-induced line broadening (37), which is caused by the sample's close proximity to the detection coil (38). Matching the magnetic susceptibility of the environment to that of the coil by use of perfluorinated organic liquids reduces the inhomogeneity of the static magnetic field in the sample region and substantially improves the line shape and resolution (39, 40).

Usually, the value of the SNR for an NMR experiment is expressed for a given analyte concentration (the standard ^{1}H sensitivity test for high-resolution NMR spectrometers is 0.1% ethylbenzene in $CDCl_3$); however, for small volumes, a better way to define the SNR is by time-normalized concentration sensitivity (S_c) (1),

$$S_c = \frac{\mathrm{SNR}}{C \times t_a^{1/2}}, \tag{3}$$

where C is the sample concentration and t_a is the total acquisition time. Similarly, the mass sensitivity (S_m) is a more appropriate way to define the probe performance when dealing with mass-limited samples:

$$S_m = \frac{\mathrm{SNR}}{m \times t_a^{1/2}}, \tag{4}$$

where m is the mass of analyte inside the observed volume.

An NMR figure of merit that must be considered if the performances of different probes are to be compared is the limit of detection (LOD). Kentgens et al. (41) defined the LOD as the number of nuclear spins that have to resonate in a bandwidth of 1 Hz to give a signal as strong as the root-mean-square noise in a single-scan experiment:

$$\mathrm{LOD} = \frac{Ns}{\mathrm{SNR}_{t,SS}\sqrt{\Delta f}}, \tag{5}$$

where N_S is the number of spins, Δ_f is the bandwidth in which the spins have to resonate, and $\mathrm{SNR}_{t,SS}$ is the single-scan SNR in the time domain.

However, in the literature, the LOD is often expressed in terms of the normalized mass ($nLOD_m$) or concentration ($nLOD_c$) of sample necessary to acquire a desired SNR for a specific peak and a given acquisition time (in the few reported examples, the anomeric peak of the sucrose is chosen to define the LOD of microcoil probes).

Constructing a probe for NMR spectroscopy is a far-from-trivial task. The perfectly optimized commercial probes are the result of a combined physics, materials science, electronics, and mechanical engineering effort (42); the design and fabrication of microcoil probes are even more challenging. For the highest possible sensitivity and resolution to be achieved, the geometry of the coil must be optimized, circuit losses and magnetic susceptibility–induced line broadening must be minimized, and the generated B_1 field must be homogeneous over the entire sample volume. The typical coil geometry used in conventional modern solution-state NMR probes is of the saddle type (**Figure 1**), which generates a very homogeneous magnetic field orthogonal to

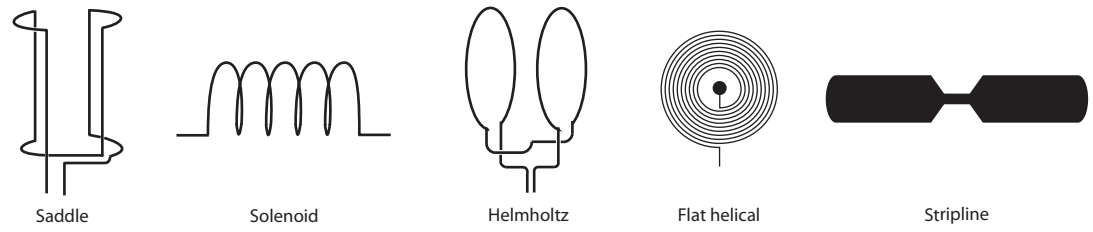

Figure 1

Possible geometries of nuclear magnetic resonance coils.

the direction of the B_0 axis. However, the saddle geometry is not very suitable for miniaturization, and for small-volume NMR coils, three main geometries have been reported: solenoidal, planar helical, and transmission-line type (microslot waveguides and striplines). In the next section, we discuss the advantages and drawbacks of each of these geometries.

3.1. Microsolenoids

Microsolenoid coils are generally fabricated by tightly winding a wire in a helical form around the sample container, which is typically a capillary. This process is an efficient way to produce a strong and homogeneous B_1 magnetic field, and because the coil closely adapts to the size and shape of the samples, a good filling factor (1, 31) is achieved.

COSY: correlation spectroscopy

The implementation of solenoidal microcoils for NMR spectroscopy and imaging has been pioneered by Sweedler and coworkers (38, 39), who designed a miniature RF coil, wrapped around a capillary, that provides a detection cell of approximately 5 nl. By using Fluorinert^{TM} FC-43 as a susceptibility-matching fluid, the authors obtained line widths of 0.6 Hz for a neat ethylbenzene sample (**Figure 2**). The LOD for sucrose was 19 ng (56 pmol) for a total acquisition time of 1 min. A two-dimensional (2D) ^{1}H-^{1}H correlation spectroscopy (COSY) spectrum of 1 μg (4.5 nmol) of 2,3-dibromopropionic acid showed all the expected cross peaks, which were in good agreement with the spectrum acquired in a normal 5-mm probe.

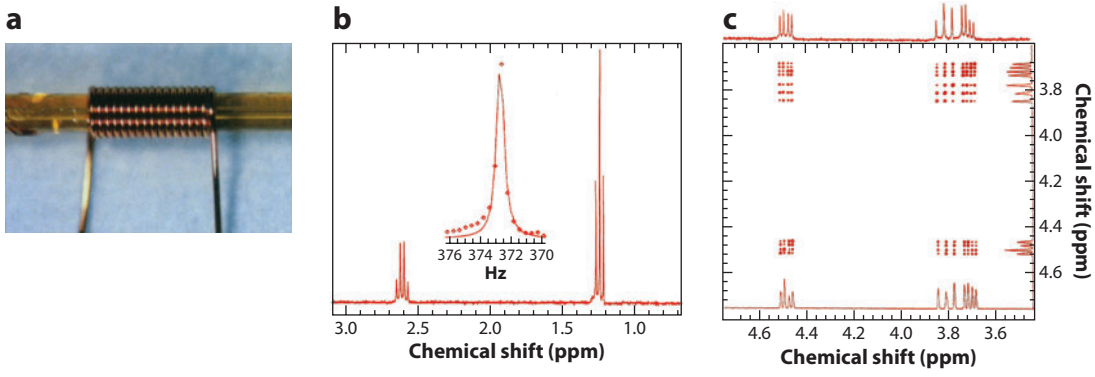

Figure 2

(*a*) Solenoidal copper microcoil wrapped around a polyimide-coated fused-silica capillary. (*b*) Microcoil ^{1}H nuclear magnetic resonance spectrum of neat ethylbenzene (4.3 μg, 31 nmol). Only the aliphatic region is displayed. (*Inset*) The line fit diagram for the central peak of the triplet. (*c*) Microcoil ^{1}H-^{1}H correlation spectroscopy spectrum of 2,3-dibromopropionic acid in acetone d_6. Reprinted from Reference 29 with permission from the American Association for the Advancement of Science.

HSQC: heteronuclear single quantum coherence

Following this promising proof of principle, the microsolenoid coil approach has found many applications both for the analysis of small amounts of sample and in the hyphenation of NMR spectroscopy to other analytical techniques (see Section 4.2). Minard & Wind (43, 44) provide detailed guidelines for the design of solenoid microcoils in terms of RF homogeneity, coil dimensions, and winding parameters. See Ciobanu et al. (45) and Neuberger & Webb (46) for an overview of solenoidal microcoils used in MRI. Most of the recent advances in microsolenoid coil fabrication and application for static submicroliter liquid-state NMR spectroscopy are discussed below.

The main drawbacks of hand-wound solenoidal microcoils are the fabrication difficulties encountered at very small dimensions, as well as accurate sample and coil positioning (47, 48). Microcontact printing represents an alternative technique to fabricate microcoils on capillaries, but these microcoils generally showed lower sensitivity than the ones fabricated by direct winding of the copper wire, probably because of their higher resistance (49). However, they showed good resolution, with line widths of less than 1 Hz for a neat 8-nl ethylbenzene sample. Malba et al. (47) introduced laser-lathe lithography, a novel method to manufacture miniature NMR coils of different designs; moreover, they integrated laser-fabricated microsolenoids in a portable NMR system with a 2-T magnet (48). Comparison between laser-lathe-fabricated microcoils and other RF probes, including a commercial 5-mm Varian probe, the Nalorac SMIDG, and a manually wound microcoil, showed that the molar sensitivity (S_M) and the molar LOD ($nLOD_M$) are significantly improved for the former. Solenoid, Helmholtz, and planar microcoils were fabricated on the same wafer through the use of microfabrication, and their performances indicate that microsolenoids are superior in terms of sensitivity and RF-field uniformity but that they have a rather low spectral resolution (50). Recently, subnanoliter solenoidal NMR transceiver coils were fabricated by multilayer soft lithography based on replica molding, and a ^{1}H-NMR spectrum for a 0.5-M D-alanine solution was acquired; however, there is room for improvement in terms of both resolution and sensitivity (51). Seeber et al. (52) obtained a single-scan ^{1}H-NMR spectrum from 10 fl (1 fl $= 10^{-12}$ l) of water contained in a micropipette with a diameter of 20 μm; the solenoidal microcoil was wrapped around the sample container via a winding apparatus.

Li et al. (53) incorporated multiple microsolenoids into the same probe head for high-throughput NMR spectroscopy. A four-coil setup with an observed volume of 28 nl for each coil was optimized for 5.9 T, which allowed the simultaneous acquisition of 1D and 2D spectra from fructose, galactose, adenosine triphosphate, and chloroquine; the resulting line widths ranged from 2 to 4 Hz. For a more compact two-coil system designed for 11.7 T and with volumes of 5 and 31 nl, respectively, better resolution (FWHM <2 Hz) was achieved. There was a minimal loss in sensitivity compared with a single coil (53); therefore, throughput increases linearly with the number of coils. This approach may offer a solution for combinatorial chemistry, which places a high demand on the analysis of multiple, often small-volume samples in a given amount of time.

Microsolenoid coils can also be successfully applied to natural-abundance ^{13}C NMR spectroscopy, as demonstrated by Subramanian & Webb (54), who designed both direct and inverse detection probes with active volumes of 1 μl and 550 nl, respectively. The LOD for natural-abundance ^{13}C direct detection is 18 μg for a total acquisition time of 90 min, whereas ^{13}C enrichment lowers the LOD to less than 1 μg. The first heteronuclear single quantum coherence (HSQC) spectrum obtained from a solenoidal microcoil was reported by the same authors, who used an inverse detection microprobe consisting of a microsolenoid and a single-turn planar microcoil as the ^{1}H and ^{13}C channels, respectively (55). The HSQC spectrum of 40 nmol of chloroquine in an observed volume of 745 nl was acquired in 3.6 h and yielded all the expected ^{1}H-^{13}C cross peaks.

A dual-microcoil, double-resonance NMR probe with thermally etched 440-nl detection volumes was recently designed (56). The two microcoils were placed orthogonally, and a double-resonance circuit was used for each coil for tuning and matching the ^{1}H-^{2}H frequencies (300 and 46.05 MHz, respectively) for the upper coil and the ^{1}H-^{13}C frequencies (300 and 75.44 MHz, respectively) for the lower one. Incorporation of the lock channel into the resonant circuit of the upper coil improved the line shape for longer 2D acquisitions on either sample coil. The coils exhibited good performance, with line widths ranging from 0.8 to 1.1 Hz and a high sensitivity for both ^{1}H and ^{13}C. Directly detected spectra (both coupled and decoupled) for ^{13}C were obtained in less than 5 min from a 5% volume/volume double ^{13}C–labeled acetic acid sample in D_2O.

3.2. Planar Microcoils

Planar microcoils are easily batch-fabricated by standard photolithographic techniques, which allow the straightforward production of features with submicrometer resolution. Moreover, photolithography allows good control of the coil geometry and is amenable to integration with chip-based microfluidic devices. Finally, microfabrication enables the production of arrays of microcoils and microfluidic channels for high-throughput NMR studies. The first planar microcoils, reported by Peck and coworkers (57), were fabricated from gold on gallium arsenide substrates and used to register the NMR spectrum of a silicone rubber sample placed directly over the coil. The low spectral resolution (360 Hz) was attributed to the magnetic susceptibility variations in the region of the coil and the sample. The use of Fluorinert^{TM} FC-43 as a susceptibility matching liquid allowed a line width of 1.8 Hz for a water sample confined in a volume of approximately 880 pl inside a capillary positioned above the coil (58). However, the ^{1}H-NMR spectrum of 440 pmol of sucrose acquired with this microcoil could not compete, in terms of resolution and SNR, with the spectrum obtained with a 5-nl solenoidal microcoil (39).

The low sensitivity of these first-generation planar microcoils is due to their high series resistance, given that the SNR for miniaturized coils is dominated by the thermal noise of the coil. Massin et al. (59) were the first to report the design and fabrication of a planar microcoil with a series resistance of less than 1 Ω. For a given sample volume and coil radius, these authors showed that the SNR depends on the geometrical parameters of the coil: the number of turns, the spacing between turns (s), and the thickness (h) and width (w) of the wire (**Figure 3**). Increasing the number of turns can increase the unitary field produced by the coil but will also lead to higher series resistance. An additional problem is that the innermost turn of the planar spiral coils must be connected to the contact pads via a wire bonding or bridge. Through the use of a three-turn, 500-μm-inner-diameter coil with $h = 12$ μm, $w = 40$ μm, and $s = 30$ μm, an SNR of 20 was measured for a single-scan ^{1}H spectrum (300 MHz, 7 T) of 160 nl of neat ethylbenzene contained in a capillary positioned above the coil (**Figure 3*a***). A further improvement to the setup—specifically, integration of microfluidic channels into the glass substrate below the microcoil—yielded an SNR of 120 per scan for a 30-nl water sample (60). The authors of a subsequent theoretical and experimental study fabricated electroplated planar microcoils integrated on glass substrates with etched microfluidic channels (**Figure 3*b***) (61). The performances of three coils with observed sample volumes of 30, 120, and 470 nl were compared in terms of SNR and resolution with the predicted values, and an increase in mass sensitivity corresponding to the reduction of the coil diameter was demonstrated.

Wensink et al. (62) reported an optimum planar coil geometry derived from finite-element simulations performed using FEMM software (see **http://www.femm.info/wiki/HomePage**). An SNR of 550 was obtained for a pure-water sample in a low-field magnet (1.4 T, corresponding to 60 MHz for ^{1}H). The coil was integrated in a glass microfluidic chip with the aim of monitoring

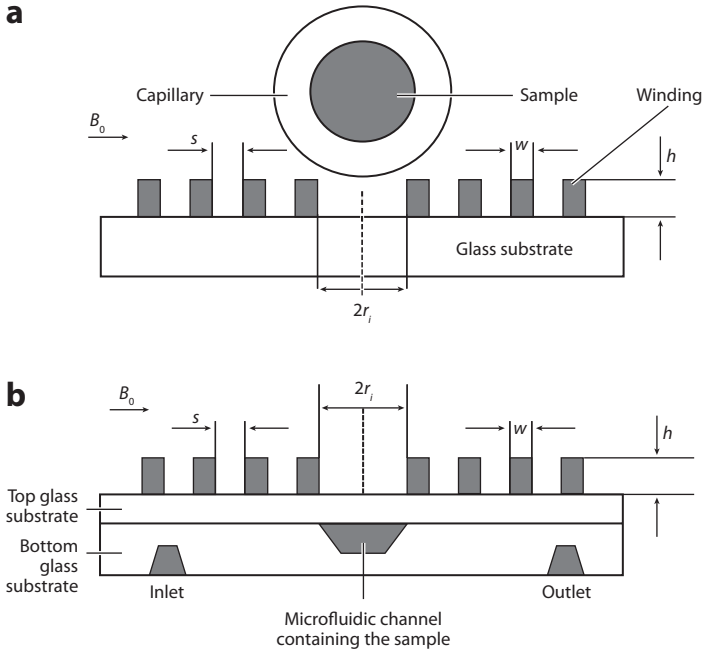

Figure 3

(*a*) Planar spiral microcoil on top of a glass substrate; the sample is contained in a capillary positioned above the coil. (*b*) Planar microcoil integrated in a double-layer glass substrate with etched microfluidic channels in the bottom. Abbreviations: B_0, static magnetic field about whose direction the nuclear magnetic moment precesses; *h*, height of the wire; *s*, spacing between turns; *w*, width of the wire.

online chemical reactions at the nanoliter scale (see Section 4.2). The setup was further optimized to function at 9.4 T (400-MHz proton Larmor frequency), which led to higher spectral resolution and sensitivity (63).

The ^{19}F nucleus offers the advantages of (*a*) a high-sensitivity, 100% natural abundance of the NMR-active (spin $= \frac{1}{2}$) isotope; (*b*) a high gyromagnetic ratio; and (*c*) a large chemical shift range compared with those of ^{1}H and ^{13}C nuclei. In addition, long-range spin-spin coupling constants of other nuclei to fluorine may have characteristic values and provide valuable connectivity information (64). Therefore, ^{19}F-NMR spectroscopy represents a useful alternative to ^{1}H-NMR for small-volume applications, as was demonstrated by Gómez et al. (65). These authors used a 50-nl active-volume microfluidic chip equipped with a planar transceiver microcoil to acquire a single-scan spectrum of octafluorotoluene with a resolution of 5 Hz, enabling the observation of long-range F-F couplings (**Figure 4**). They also investigated the host-guest interaction between $NaPF_6$ and α-cyclodextrin; thermodynamic data (association constant) and complex stoichiometry (Job's Plot) were obtained from concentration ranges and titration studies that had the same accuracy as in a normal 5-mm NMR tube.

Leidich et al. (66) designed a hybrid microdetector, with active volumes ranging from 5 to 40 nl, for high-resolution ^{1}H-NMR spectroscopy at 750 MHz (17.6 T). This detector, known as a silicon cylinder spiral coil, consists of several silicon and planar coil layers positioned in a Helmholtz-like manner and connected via bond wires. A glass capillary situated in the central bore of the detector allows for the sample spinning. Using a dual–coil layer configuration with an active volume of 36 nl, the authors obtained FWHM line widths of less than 2 Hz for an ethanol

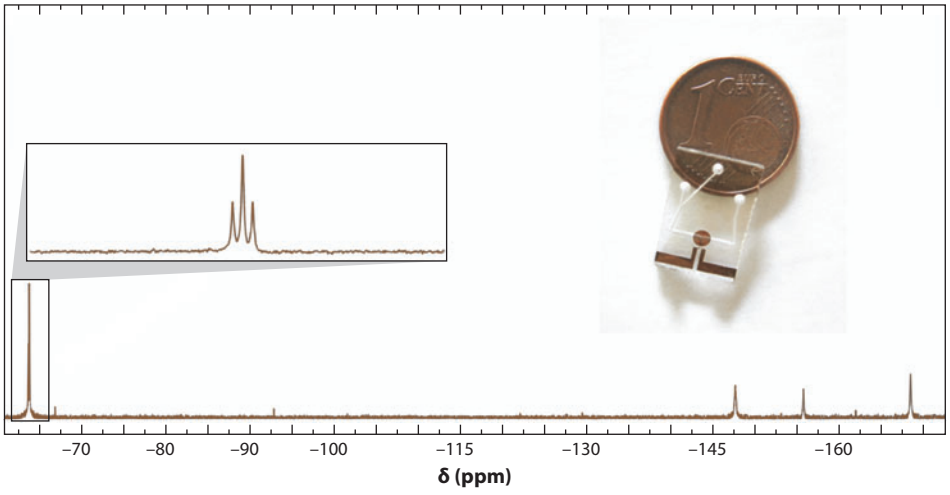

Figure 4

Single-scan ^{19}F nuclear magnetic resonance spectrum of octafluorotoluene (0.35 mmol in 50 nl of dimethyl sulfoxide). Reproduced from Reference 65 with permission. Copyright 2008, Wiley.

sample without rotating it; however, for single–coil layer designs with volumes of 13 and 5 nl, the sample had to be spun to achieve reasonably narrow lines.

A major advantage of the planar coil geometry is that it is possible to integrate several coils and the corresponding electronic components into a single-chip array. This approach could be extremely useful for parallel NMR spectroscopy and imaging. Boero and coworkers (67) reported a first single-chip array of NMR receivers, composed of eight separate channels. Each channel has a planar square detection coil with a cross section of 500 μm, which results in a densely packed array with a total area of 1 mm by 2 mm. The excitation coil is a single-turn planar coil surrounding the array, and the entire setup is optimized for operation at 300 MHz. The resolution achieved without the use of a susceptibility-matching fluid was 4 Hz (FWHM) for water samples of 12 and 55 nl; although this value must be improved for spectroscopic applications, it is sufficient for most imaging purposes.

3.3. Microslot Waveguides and Stripline Microprobes

A completely new microprobe geometry, comprising a thin-strip conductor and a ground plane separated by a low-loss dielectric material, was introduced in 2001 by Zhang et al. (68) for high-field in vivo MRI applications. Maguire et al. (69) recently used the planar microslot waveguide geometry for NMR spectroscopy microprobes (**Figure 5**). The coil design, which is based on a dual-layer metallic microstrip, is scalable to submicrometer dimensions and is easy to fabricate in parallel arrays. Moreover, the field lines in the vicinity of the microslot are more homogeneous than the field lines produced by a planar spiral coil or a metallic wire. The microslot waveguide yields (*a*) a line width of 1.1 Hz for a water sample, without requiring the use of a susceptibility-matching fluid, and (*b*) an SNR of 984 for the anomeric proton of sucrose (15.6 nmol)—the highest value reported for a planar microprobe. The good sensitivity of the microslot geometry was further demonstrated through comparison of 1D and 2D (^1H-^1H COSY) spectra of a ribonuclease A solution at a concentration of 8.3 mM in the microslot probe (188 nl, 1.57 nmol) and in a conventional Nalorac 5-mm probe (660 μl, 5.48 μmol).

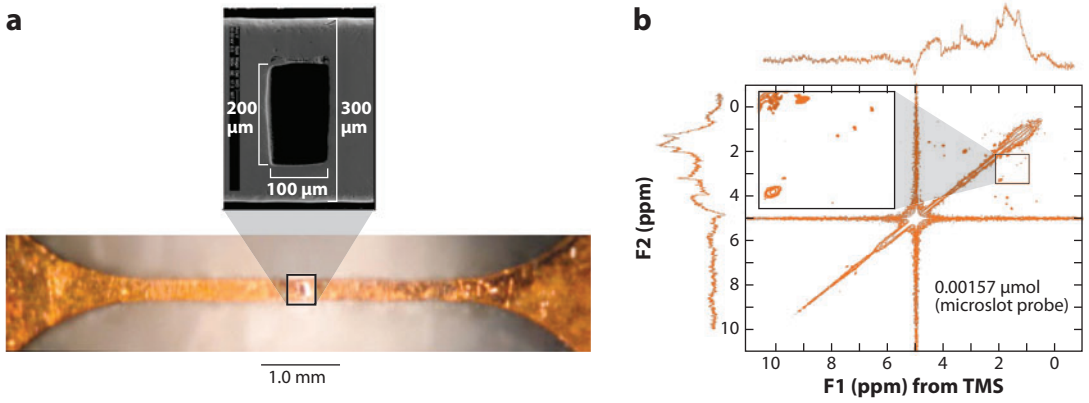

Figure 5

(*a*) Picture of the microslot, fabricated using a 248-nm excimer laser. (*b*) Two-dimensional correlation spectroscopy spectrum of protein ribonuclease A acquired in the microslot probe (1.57 nmol). Abbreviation: TMS, tetramethylsilane. Reproduced from Reference 69 with permission. Copyright 2007, National Academy of Sciences, USA.

Krojanski et al. (70) designed a similar microslot probe with an effective volume of 10.6 nl for use in metabolomics studies; this probe has $nLOD_M$s of 0.39 nmol for sucrose and 0.68 nmol for lactate. Moreover, 2D experiments such as COSY and TOCSY (total correlation spectroscopy) could yield reasonable resolution even when using five-orders-of-magnitude-less sample than is required for a conventional NMR probe. A ^{1}H-NMR spectrum of metabolite concentrate from a noncancer colon mucosa cell line (NCM 460) acquired in the microslot probe showed significantly broader signals than in a commercial probe because of the absence of the lock circuit and susceptibility matching; and low-intensity peaks were not observed. However, with further improvements, the microslot NMR probe could become a cheap alternative for metabolomics studies.

The stripline design, introduced in 2004 by Kentgens and coworkers (71), has the advantage of a nonradiative, closed configuration, compared with the microslot. This configuration is obtained by placing symmetric ground planes above and below the stripline. As a consequence, the B_1 field lines are parallel to the stripline surface, which results in a large volume with a homogeneous magnetic field and fewer electrical losses (72). The stripline detector demonstrated high sensitivity and spectral resolution (line widths of less than 1 Hz for a sample of 600 nl of pure ethanol) without the necessity of additional susceptibility matching (41). To test the potential of the stripline probe for metabolomics applications, ^{1}H-NMR spectra of human cerebrospinal fluid were acquired in a commercial 5-mm probe and in the stripline probe (73). Again, the absence of a lock channel resulted in slightly broader signals for the stripline, but most of the metabolites in the aliphatic region of the spectrum were easily identified (**Figure 6*b***). Further optimization of the stripline-based microfluidic chip afforded a RF homogeneity of 76%, which was comparable to that obtained for commercial liquid-state NMR probes (74), and allowed high-resolution 1D (600 nmol sucrose in D_2O) and 2D ^{1}H-^{1}H COSY (1.2 µmol glucose) spectra to be acquired.

4. HYPHENATED SMALL-VOLUME NUCLEAR MAGNETIC RESONANCE SYSTEMS

In association with the ability to perform synthetic and analytical processes in lab-on-a-chip devices, rapid developments in miniaturization are taking place. Carrying out laboratory operations

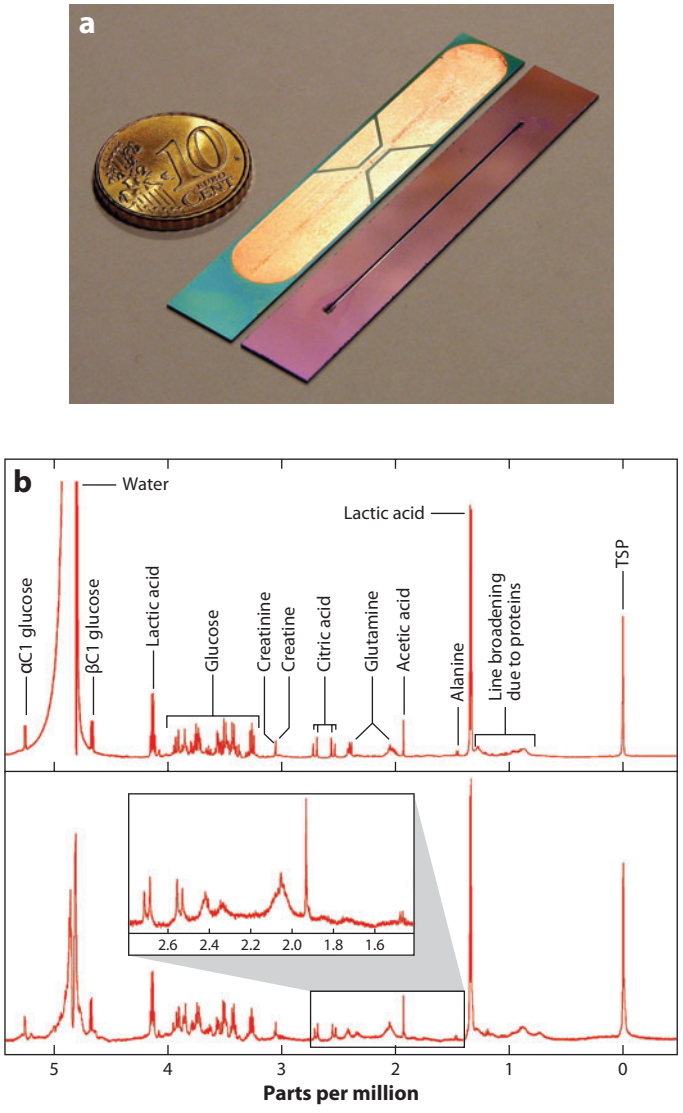

Figure 6

(*a*) The two halves of a microfluidic nuclear magnetic resonance (NMR) chip, based on the stripline design, that represent the construction of the λ/2 resonator and the microfluidic channel, respectively. The two halves are bonded together in the final device. Reprinted with permission from Reference 41. Copyright 2008, American Institute of Physics. (*b*) ^{1}H-NMR spectra of human cerebrospinal fluid recorded in (*top*) a 5-mm NMR tube and (*bottom*) the microfluidic NMR chip. Abbreviation: TSP, 3-(trimethylsilyl)-2,2-3,3-tetradeuteropropionic acid. Reprinted with permission from Reference 73. Copyright 2009, American Chemical Society.

at small scales and integrating the synthetic and analytical steps in the same device are extremely appealing prospects. In so doing, the amounts of reagents and chemical waste are much reduced, which makes the whole process safer, cheaper, and more environmentally friendly. Small volumes also reduce the times needed for the synthesis and analysis of a compound, thereby enabling parallel synthesis and high-throughput chemistry.

CAPILLARY ISOTACHOPHORESIS

In cITP, the sample is inserted between a leading electrolyte, which has a high electrophoretic mobility, and a trailing electrolyte, which has a low electrophoretic mobility. The application of an electric field induces the formation of sharp, stable boundaries between regions of ions with different mobilities. Once formed, these zones travel at a constant velocity through the separation channel. To maintain a constant current, each zone must expand or contract so that its concentration is proportional to that of the leading electrolyte.

Over the past two decades, the number of applications of micro total analysis systems (μTAS) has continuously increased; these applications range from synthetic and analytical chemistry to proteomics, immunoassays, DNA analysis, and so on (75–81). Detection represents one of the main challenges for the miniaturization of analytical systems because very sensitive techniques are required for the analysis of ultrasmall samples (82). Laser-induced fluorescence, electrochemical detection, and mass spectrometry are the three main detection techniques employed in μTAS. Less commonly used techniques include IR, UV, and surface-enhanced Raman spectroscopies; surface plasmon resonance; and thermal lens microscopy. In the next two sections, we highlight some applications of small-volume NMR spectroscopy to hyphenation with miniaturized analytical systems and describe the integration of this technique with lab-on-a-chip platforms and microreactors.

In a systematic study, Laude & Wilkins (83) showed that, to obtain maximum sensitivity and resolution for on-flow experiments, flow rates must be carefully optimized. On one hand, the analyte flow through the coil leads to a shorter longitudinal relaxation time ($T_{1,flow}$), thereby allowing for more rapid pulse repetition and an increase in the SNR per unit time. On the other hand, the transverse relaxation time ($T_{2,flow}$) is also shorter because not all spins remain in the detection cell for the entire data-acquisition time; as $T_{2,flow}$ is inversely related to the line width, working on-flow induces line broadening.

4.1. Nuclear Magnetic Resonance Detection Coupled to Separation Techniques

Hyphenated analytical techniques have become common tools in many areas of analytical chemistry, including drug-metabolite identification, food chemistry, and polymer science. To date, conventional NMR spectroscopy has been coupled to gas chromatography, supercritical fluid chromatography, gel-permeation chromatography, high-performance liquid chromatography (HPLC), capillary electrophoresis (CE), and capillary isotachophoresis (cITP; see the sidebar) (84–92). Below, we focus on the applications of nanoliter-range NMR spectroscopy coupled to HPLC and CE.

μTAS: micro total analysis system

HPLC: high-performance liquid chromatography

CE: capillary electrophoresis

4.1.1. High-performance liquid chromatography–nuclear magnetic resonance spectroscopy. In a preliminary study, Wu et al. (93) employed HPLC-NMR to separate and detect amino acids and peptides in a 50-nl-volume cell, using both static and online NMR measurements. The authors fabricated the solenoidal microcoil by winding the copper wire directly onto a fused-silica capillary, which ensured a filling factor of approximately 50%. The line widths achieved were in the range between 7 and 15 Hz, which represents a serious limitation for complex structure elucidations. Surprisingly, this is the only example of the application of nanoliter-volume solenoidal microcoils in an HPLC-NMR setup; there are few other reports of the use of low-microliter-range microsolenoids (94, 95).

An alternative approach is based on the use of capillaries placed vertically in a modified microprobe with a saddle-type RF coil, which is typically 1.2 cm long (96, 97). Because the shim system for high-field modern NMR spectrometers is optimized for saddle-type coils, this design has the advantage of a better spectral resolution but has the drawback of a low filling factor, due to the significant difference between the diameter of the capillary and that of the coil. The capillary HPLC–NMR technique has been successfully applied to the analysis of nanomolar amounts of different natural products, for instance, the structural elucidation of a new retinyl acetate dimer using 1D and 2D NMR experiments (98).

4.1.2. Capillary electrophoresis–nuclear magnetic resonance spectroscopy. CE is a highly efficient, versatile separation technique based on the electrophoretic mobility of analytes (99), and CE microchips are one of the earliest examples of a μTAS system (100). The first application of ^{1}H-NMR spectroscopy for the online detection in CE separation of amino acids was reported in 1994 by Wu et al. (30, 38). The authors tested different submicroliter-volume (5-, 50-, and 200-nl) NMR detection cells that consisted of solenoidal microcoils wrapped around capillaries. Although the LOD_m did not improve with the use of larger coils, the LOD_c improved significantly. In a comprehensive study, Olson et al. (101) showed that the application of CE voltages produces a large perturbation in the NMR signals, especially when the capillary containing the sample and the static magnetic field are not parallel. To alleviate this effect, the authors used a periodic stopped-flow approach: CE voltage was applied for 15 s, then stopped for 1 min to register the NMR spectrum, and then the whole procedure was repeated. The effect of the magnetic field gradients induced by the electrophoretic current was thereby eliminated, and the spectral resolution and the sensitivity of the NMR experiment increased. The use of a dual-microcoil setup allowed continuous CE separation in which the electrophoretic flow was directed toward two different outlet capillaries, each of which had its own microcoil with a detection volume of 25 nl (102). Stopped-flow NMR data were acquired from one coil, while the second coil was filled with new analyte from the CE separation.

The dual-microcoil NMR-CE coupling has been applied to the analysis of less than 3 nmol of a mixture of two amines; FWHM values of 1 to 2 Hz were obtained. In a similar approach, a cyclic CE system was coupled to two 5-nl-detection-volume microcoils to perform CE in closed loops (103). A two-loop, five-junction capillary configuration allowed the analytes to be directed around or between the loops; in this way, a particular analyte band was detected in one coil while CE continued in the second loop and was monitored by the second NMR coil. This method was used to separate alanine, valine, and threonine, and their 1D and 2D spectra were acquired under stopped-flow conditions in the absence of the applied voltage (**Figure 7**).

Sweedler and coworkers (104) used cITP for sample concentration prior to NMR analysis. cITP coupled to a 30-nl NMR solenoidal microprobe allowed the analysis of a mixture of tetraethylammonium bromide, methyl green, and the dipeptide alanine-lysine, each of which was injected at a concentration of 200 μM. A 100-fold increase in sample concentration was obtained, which enabled the acquisition of ^{1}H-NMR spectra in less than 1 min. The usefulness of the cITP-NMR coupling was also demonstrated for trace impurity measurements. In this experiment, the investigators used a 200-μM solution of atenolol in a 1,000-fold excess of sucrose (105), and the concentration sensitivity of the microcoil probe approached that of commercial 5-mm NMR probes. The small volumes required for cITP are also an advantage in the separation of enantiomers involving expensive chiral additives and their posterior structural analysis (106, 107).

The small-volume saddle-type RF coil developed for the capillary HPLC–NMR coupling (see Section 4.1.1) was also successfully applied to CEC (capillary electrophoresis and

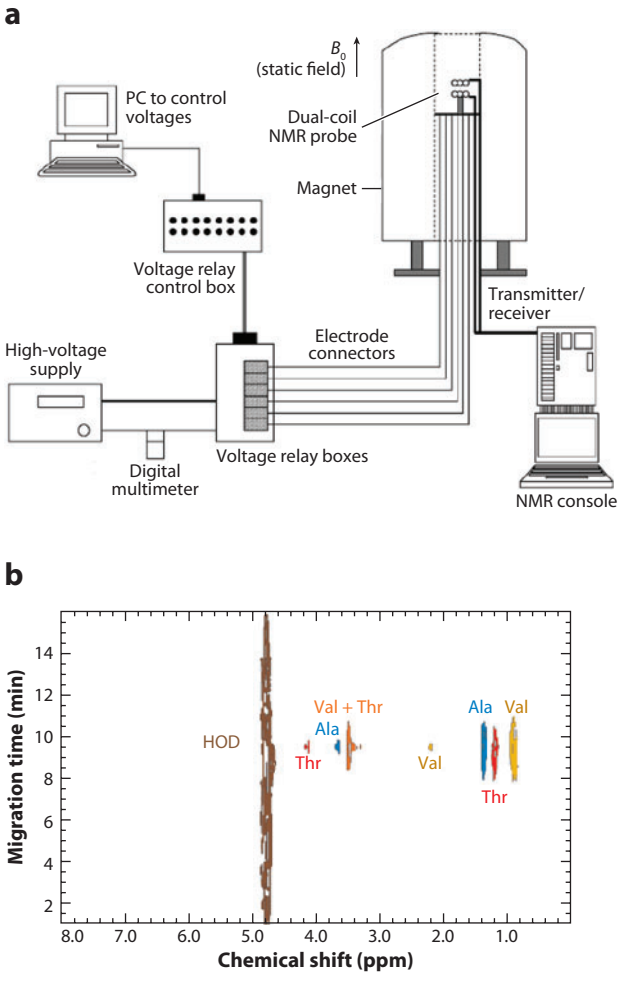

Figure 7

(*a*) Detailed instrumental arrangement used for cyclic capillary electrophoresis–nuclear magnetic resonance spectroscopy (CE-NMR) in an NMR probe, illustrating the control circuitry used. (*b*) Two-dimensional CE-NMR electropherogram (chemical shift versus migration time) for the separation of alanine (Ala), valine (Val), and threonine (Thr). Abbreviation: HOD, hydrogen deuterium oxide. Reprinted with permission from Reference 103. Copyright 2004, American Chemical Society.

electrochromatography) (108, 109). In these studies, enlarged detection cells of 240 and 400 nl were used, which ensured a higher residence time of the analyte. Separation and identification of paracetamol metabolites from human urine were performed at submicroliter volumes by coupling CE and CEC to NMR spectroscopy (109).

On-chip integration of CE and NMR can be performed using planar microcoils, as was demonstrated by Trumbull et al. (110). Although the SNR of 23.5 per scan and the line width of 1.4 Hz obtained for a 30-nl sample of water are adequate for the detection of analytes at high concentration, the use of planar microcoils is not practical at the very low concentrations typically employed for CE.

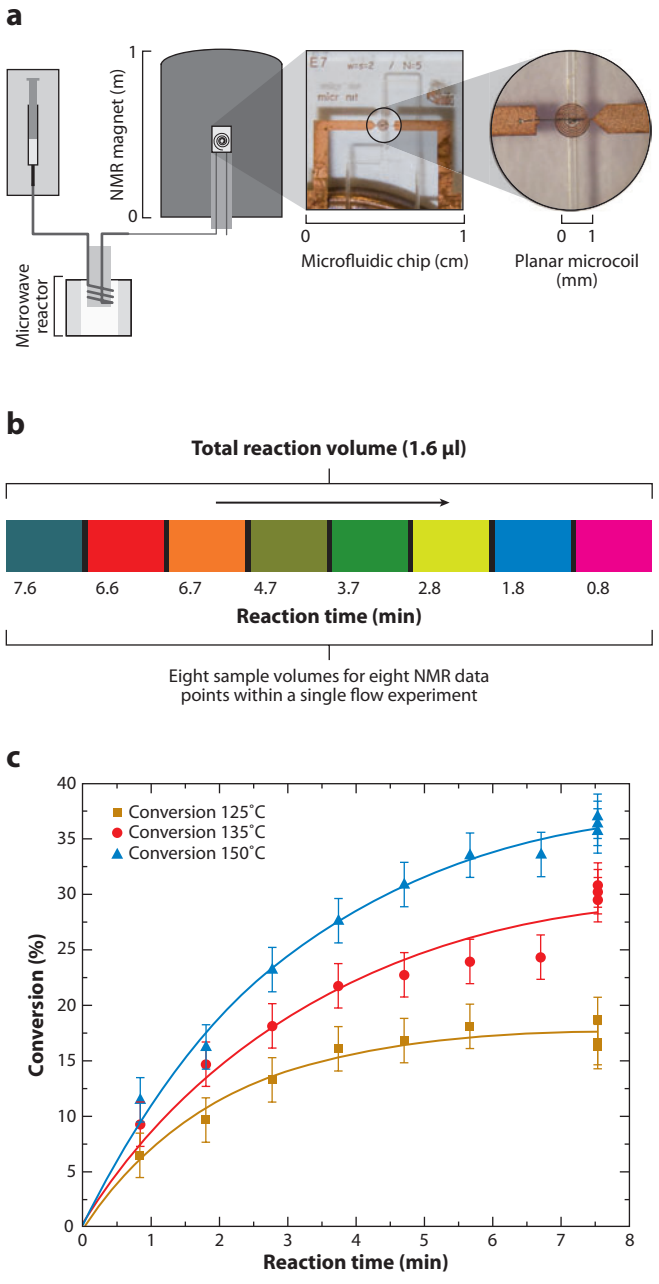

Figure 8

(*a*) (*Left*) Hyphenated syringe-microwave-NMR (nuclear magnetic resonance) setup. (*Middle*) Zoomed-in view of the microfluidic NMR chip. (*Right*) The integrated planar radio frequency transceiver microcoil on top of the 200-µm-wide fluidic channel. (*b*) The eight sample portions of the reaction volume were exposed to the microwave irradiation for different times and analyzed successively in a single 2-µl flow experiment. The arrow indicates the direction of the flow. (*c*) Conversion of the cycloaddition reaction product versus reaction time for three different temperatures. Reproduced from Reference 114 with permission from the Royal Society of Chemistry.

4.2. Integration of Nuclear Magnetic Resonance Spectroscopy with Lab-on-a-Chip Devices and Microreactors

Microreactors allow for the use of minimal amounts of reagents under precisely controlled conditions, and they are well suited for rapid screening of reaction conditions and kinetics studies (111). Kakuta et al. (112) coupled a micromixer and a solenoidal NMR microcoil (with a detection volume of 800 nl) to study real-time methanol-induced conformational changes of ubiquitin on a timescale of seconds. Sweedler and colleagues (113) used a multiple-microcoil NMR setup to study the kinetics of D-xylose-borate reaction by NMR spectroscopy. The two reagents were mixed in a Y-shaped mixer, then passed through a capillary around which three identical solenoidal microcoils (each of which had a detection volume of approximately 31 nl) were wrapped. The reaction times were determined by the combination of the flow rates and the distance between the mixer and each NMR microcoil. Bart et al. (73) employed a glass microreactor coupled to a stripline NMR chip with a detection volume of 600 nl for the real-time monitoring of the acetylation of benzyl alcohol with acetyl chloride in the presence of *N,N*-diisopropylethylamine. The ^{1}H-NMR spectra recorded on-flow allowed for the detection of reaction intermediates, which were almost unobservable when the reaction was performed in a 5-mm NMR tube.

Recently, microwave-assisted continuous-flow organic synthesis was hyphenated with nanoliter-volume NMR spectroscopy; this combination is a promising tool for the rapid optimization of reaction conditions (114). In this experiment a fused-silica capillary was wrapped around a Weflon^{TM} bar, yielding a reaction volume of 1.6 μl, and coupled to a microfluidic NMR chip equipped with a planar transceiver microcoil (with a detection volume of 6 nl). A Diels-Alder cycloaddition was chosen as the model reaction, and the conversion was calculated at three different temperatures. Because the volume of the NMR chip is much lower than the microwave reaction volume, the latter can be divided into several zones (**Figure 8*b***); under flow conditions, each of these zones is exposed to the microwave irradiation for different times. By choosing the appropriate flow rate and the NMR acquisition parameters, the necessary data points for determining the conversion were obtained in a single constant-flow experiment.

The only fully integrated μTAS-NMR setup reported to date was used by Wensink et al. (115) for a kinetic study of the imine formation from aniline and benzaldehyde by ^{1}H-NMR spectroscopy at 1.4 T. A planar microcoil was integrated on top of a microfluidic chip containing two inlets, a mixing zone, a detection zone, and one outlet; the total channel volume between the mixing point and the coil was 0.57 μl, and the detection volume was 56 nl. The residence time in the detection volume ranged from 0.9 s to 30 min, depending on the flow rate.

5. CONCLUSIONS AND PERSPECTIVES

Over the past two decades, miniaturized RF coils have been successfully implemented for the analysis of small sample volumes by NMR spectroscopy; they have also been used for hyphenation with other analytical techniques and have been integrated with microfluidic devices and microreactors. Different coil geometries have been employed mainly for ^{1}H and ^{13}C mono- and bidimensional experiments, but detection of other high-sensitivity nuclei (e.g. ^{19}F) is also possible. Nanoliter-volume NMR spectroscopy research is still in an early stage, and hopefully, future technical improvements will lead to novel applications. On one hand, combining the microcoil approach with other sensitivity-enhancement schemes, such as polarization transfer or cryogenic cooling, should result in further improvements in the sensitivity of NMR experiments for small-volume samples. On the other hand, nanoliter-volume microcoils can be used in miniaturized tabletop and portable NMR systems operating at low fields (116). Miniaturized coils are also suitable for use in high-field magnets because of their less stringent homogeneity requirements,

compared with commercial probes (117). The potential of planar microcoils for lab-on-a-chip applications has yet to be fully explored; for example, integration of multiple planar microcoils on the same microfluidic chip would enable high-throughput studies as well as heteronuclear and/or 2D experiments, and a sample-cooling and -heating mechanism could be incorporated for variable-temperature experiments. We anticipate that high-resolution small-volume NMR spectroscopy will become an active research field in the coming decades.

SUMMARY POINTS

1. Miniaturization of RF coils represents an effective way to enhance the sensitivity of NMR spectroscopy for mass- and volume-limited samples.
2. Microsolenoidal coils are extremely versatile in terms of applications (^{1}H and ^{13}C, mono- and bidimensional NMR experiments, multiple coil designs for high-throughput analysis, NMR spectroscopy hyphenated with separation techniques) and offer good sensitivity, but they are not easy to batch-fabricate, especially in very small dimensions.
3. The planar microcoil geometry is ideal for straightforward fabrication through the use of photolithography, and it holds great promise for the integration of NMR spectroscopy with lab-on-a-chip devices; however, the sensitivity of planar microcoil probes is lower than that reported for other geometries.
4. Microslots and stripline geometries combine high sensitivity and resolution with scalability, and they will probably have many future applications for NMR spectroscopy. Fabrication procedures for this type of microcoil need to be optimized to allow broad use.
5. Coil miniaturization allows the use of NMR spectroscopy in conjunction with separation techniques (e.g., HPLC, CE) for the analysis of extremely small sample volumes.
6. Microfabricated NMR detectors have been successfully hyphenated and/or integrated with lab-on-a-chip platforms, which has enabled real-time monitoring of chemical reactions performed in microfluidic devices.

FUTURE ISSUES

1. Miniaturization of NMR coils should be combined with other sensitivity-enhancement techniques, such as DNP.
2. Detection of other NMR-active nuclei (e.g., ^{15}N, ^{31}P, ^{195}Pt) should be addressed.
3. Submicroliter-volume probes must be further optimized to achieve a performance similar to that of commercially available microprobes (>1 μl).
4. Integration of a lock channel for more advanced NMR experiments and long-time measurements is necessary.
5. Multicoil setups should be developed and implemented to allow more complex pulse sequences, as well as heteronuclear and multidimensional NMR experiments.
6. Fully miniaturized tabletop and portable low-field NMR systems that incorporate microcoil probes should be constructed.

DISCLOSURE STATEMENT

The authors are not aware of any affiliations, memberships, funding, or financial holdings that might be perceived as affecting the objectivity of this review.

LITERATURE CITED

1. Lacey ME, Subramanian R, Olson DL, Webb AG, Sweedler JV. 1999. High-resolution NMR spectroscopy of sample volumes from 1 nl to 10 μl. *Chem. Rev.* 99:3133–52
2. Abragam A. 1961. *The Principles of Nuclear Magnetism*. Oxford, UK: Oxford Univ. Press. 614 pp.
3. Hoult DI, Richards RE. 1976. The signal-to-noise ratio of the nuclear magnetic resonance experiment. *J. Magn. Reson.* 24:71–85
4. Rinaldi PL. 2004. Three-dimensional solution NMR spectroscopy of complex structures and mixtures. *Analyst* 129:687–99
5. Schroeder FC, Gronquist M. 2006. Extending the scope of NMR spectroscopy with microcoil probes. *Angew. Chem. Int. Ed.* 45:7122–31
6. Spraul M, Freund AS, Nast RE, Withers RS, Maas WE, Corcoran O. 2003. Advancing NMR sensitivity for LC-NMR-MS using a cryoflow probe: application to the analysis of acetaminophen metabolites in urine. *Anal. Chem.* 75:1536–41
7. Brey WW, Edison AS, Nast RE, Rocca JR, Saha S, Withers RS. 2006. Design, construction, and validation of a 1-mm triple-resonance high-temperature-superconducting probe for NMR. *J. Magn. Reson.* 179:290–93
8. Fellenberg M, Çoksezen A, Meyer B. 2010. Characterization of picomole amounts of oligosaccharides from glycoproteins by ^{1}H NMR spectroscopy. *Angew. Chem. Int. Ed.* 49:2630–33
9. Long HW, Gaede HC, Shore J, Reven L, Bowers CR, et al. 1993. High-field cross polarization NMR from laser-polarized xenon to a polymer surface. *J. Am. Chem. Soc.* 115:8491–92
10. Navon G, Song YQ, Room T, Appelt S, Taylor RE, Pines A. 1996. Enhancement of solution NMR and MRI with laser-polarized xenon. *Science* 271:1848–51
11. Fitzgerald RJ, Sauer KL, Happer W. 1998. Cross-relaxation in laser-polarized liquid xenon. *Chem. Phys. Lett.* 284:87–92
12. Bowers CR, Weitekamp DP. 1986. Transformation of symmetrization order to nuclear-spin magnetization by chemical reaction and nuclear magnetic resonance. *Phys. Rev. Lett.* 57:2645
13. Joachim B. 2006. The discovery of chemically induced dynamic polarization (CIDNP). *Helv. Chim. Acta* 89:2082–102
14. Kaptein R, Dijkstra K, Nicolay K. 1978. Laser photo-CIDNP as a surface probe for proteins in solution. *Nature* 274:293–94
15. Eisenschmid TC, Kirss RU, Deutsch PP, Hommeltoft SI, Eisenberg R, et al. 1987. Para hydrogen induced polarization in hydrogenation reactions. *J. Am. Chem. Soc.* 109:8089–91
16. Pravica MG, Weitekamp DP. 1988. Net NMR alignment by adiabatic transport of parahydrogen addition products to high magnetic field. *Chem. Phys. Lett.* 145:255–58
17. Wood NJ, Brannigan JA, Duckett SB, Heath SL, Wagstaff J. 2007. Detection of picomole amounts of biological substrates by para-hydrogen-enhanced NMR methods in conjunction with a suitable receptor complex. *J. Am. Chem. Soc.* 129:11012–13
18. Becerra LR, Gerfen GJ, Temkin RJ, Singel DJ, Griffen RG. 1993. Dynamic nuclear polarization with a cyclotron resonance maser at 5 T. *Phys. Rev. Lett.* 71:3561–64
19. Ardenkjaer-Larsen JH, Fridlund B, Gram A, Hansson G, Hansson L, et al. 2003. Increase in signal-to-noise ratio of >10,000 times in liquid-state NMR. *Proc. Natl. Acad. Sci. USA* 100:10158–63
20. Bajaj VS, Farrar CT, Hornstein MK, Mastovsky I, Vieregg J, et al. 2003. Dynamic nuclear polarization at 9 T using a novel 250 GHz gyrotron microwave source. *J. Magn. Reson.* 160:85–90
21. Denysenkov V, Prandolini MJ, Gafurov M, Sezer D, Endeward B, Prisner TF. 2010. Liquid state DNP using a 260 GHz high power gyrotron. *Phys. Chem. Chem. Phys.* 12:5786–90
22. Moule AJ, Spence MM, Han S-I, Seeley JA, Pierce KL, et al. 2003. Amplification of xenon NMR and MRI by remote detection. *Proc. Natl. Acad. Sci. USA* 100:9122–27

23. Granwehr J, Seeley JA. 2006. Sensitivity quantification of remote detection NMR and MRI. *J. Magn. Reson.* 179:280–89
24. Harel E, Schröder L, Xu S. 2008. Novel detection schemes of nuclear magnetic resonance and magnetic resonance imaging: applications from analytical chemistry to molecular sensors. *Annu. Rev. Anal. Chem.* 1:133–63
25. Hilty C, McDonnell EE, Granwehr J, Pierce KL, Han S-I, Pines A. 2005. Microfluidic gas-flow profiling using remote-detection NMR. *Proc. Natl. Acad. Sci. USA* 102:14960–63
26. McDonnell EE, Han S, Hilty C, Pierce KL, Pines A. 2005. NMR analysis on microfluidic devices by remote detection. *Anal. Chem.* 77:8109–14
27. Harel E, Pines A. 2008. Spectrally resolved flow imaging of fluids inside a microfluidic chip with ultrahigh time resolution. *J. Magn. Reson.* 193:199–206
28. Telkki VV, Zhivonitko VV, Ahola S, Kovtunov KV, Jokisaari J, Koptyug IV. 2010. Microfluidic gas-flow imaging utilizing parahydrogen-induced polarization and remote-detection NMR. *Angew. Chem. Int. Ed.* 49:8363–66
29. Paulsen J, Bajaj VS, Pines A. 2010. Compressed sensing of remotely detected MRI velocimetry in microfluidics. *J. Magn. Reson.* 205:196–201
30. Wu N, Peck TL, Webb AG, Magin RL, Sweedler JV. 1994. ^{1}H-NMR spectroscopy on the nanoliter scale for static and online measurements. *Anal. Chem.* 66:3849–57
31. Olson DL, Norcross JA, O'Neil-Johnson M, Molitor PF, Detlefsen DJ, et al. 2004. Microflow NMR: concepts and capabilities. *Anal. Chem.* 76:2966–74
32. Walton JH, de Ropp JS, Shutov MV, Goloshevsky AG, McCarthy MJ, et al. 2003. A micromachined double-tuned NMR microprobe. *Anal. Chem.* 75:5030–36
33. Schlotterbeck G, Ross A, Hochstrasser R, Senn H, Kühn T, et al. 2002. High-resolution capillary tube NMR. A miniaturized 5 μl high-sensitivity TXI probe for mass-limited samples, off-line LC NMR, and HT NMR. *Anal. Chem.* 74:4464–71
34. Jansma A, Chuan T, Albrecht RW, Olson DL, Peck TL, Geierstanger BH. 2005. Automated microflow NMR: routine analysis of five-microliter samples. *Anal. Chem.* 77:6509–15
35. Webb AG. 2005. Microcoil nuclear magnetic resonance spectroscopy. *J. Pharm. Biomed. Anal.* 38:892–903
36. Webb AG. 1997. Radiofrequency microcoils in magnetic resonance. *Prog. Nucl. Magn. Reson. Spectrosc.* 31:1–42
37. Fuks LF, Huang FSC, Carter CM, Edelstein WA, Roemer PB. 1992. Susceptibility, lineshape, and shimming in high-resolution NMR. *J. Magn. Reson.* 100:229–42
38. Wu N, Peck TL, Webb AG, Magin RL, Sweedler JV. 1994. Nanoliter volume sample cells for ^{1}H NMR: application to online detection in capillary electrophoresis. *J. Am. Chem. Soc.* 116:7929–30
39. Olson DL, Peck TL, Webb AG, Magin RL, Sweedler JV. 1995. High-resolution microcoil ^{1}H-NMR for mass-limited, nanoliter-volume samples. *Science* 270:1967–70
40. Behnia B, Webb AG. 1998. Limited-sample NMR using solenoidal microcoils, perfluorocarbon plugs, and capillary spinning. *Anal. Chem.* 70:5326–31
41. Kentgens APM, Bart J, van Bentum PJM, Brinkmann A, van Eck ERH, et al. 2008. High-resolution liquid- and solid-state nuclear magnetic resonance of nanoliter sample volumes using microcoil detectors. *J. Chem. Phys.* 128:052202
42. Doty FD. 2007. Probe design and construction. In *Encyclopedia of Magnetic Resonance*, ed. RK Harris, R Wasylishen. New York: Wiley. doi: 10.1002/9780470034590.emrstm0414
43. Minard KR, Wind RA. 2001. Solenoidal microcoil design. Part I: Optimizing RF homogeneity and coil dimensions. *Concepts Magn. Reson.* 13:128–42
44. Minard KR, Wind RA. 2001. Solenoidal microcoil design. Part II: Optimizing winding parameters for maximum signal-to-noise performance. *Concepts Magn. Reson.* 13:190–210
45. Ciobanu L, Webb AG, Pennington CH. 2003. Magnetic resonance imaging of biological cells. *Prog. Nucl. Magn. Reson. Spectrosc.* 42:69–93
46. Neuberger T, Webb A. 2009. Radiofrequency coils for magnetic resonance microscopy. *Nucl. Magn. Reson. Biomed.* 22:975–81

47. Malba V, Maxwell R, Evans LB, Bernhardt AF, Cosman M, Yan K. 2003. Laser-lathe lithography—a novel method for manufacturing nuclear magnetic resonance microcoils. *Biomed. Microdevices* 5:21–27
48. Demas V, Herberg JL, Malba V, Bernhardt A, Evans L, et al. 2007. Portable, low-cost NMR with laser-lathe lithography produced microcoils. *J. Magn. Reson.* 189:121–29
49. Rogers JA, Jackman RJ, Whitesides GM, Olson DL, Sweedler JV. 1997. Using microcontact printing to fabricate microcoils on capillaries for high resolution proton nuclear magnetic resonance on nanoliter volumes. *Appl. Phys. Lett.* 70:2464–66
50. Ehrmann K, Saillen N, Vincent F, Stettler M, Jordan M, et al. 2007. Microfabricated solenoids and Helmholtz coils for NMR spectroscopy of mammalian cells. *Lab Chip* 7:373–80
51. Lam MCH, Homenuke MA, Michal CA, Hansen CL. 2009. Sub-nanoliter nuclear magnetic resonance coils fabricated with multilayer soft lithography. *J. Micromech. Microeng.* 19:095001
52. Seeber DA, Cooper RL, Ciobanu L, Pennington CH. 2001. Design and testing of high sensitivity microreceiver coil apparatus for nuclear magnetic resonance and imaging. *Rev. Sci. Instrum.* 72:2171–79
53. Li Y, Wolters AM, Malawey PV, Sweedler JV, Webb AG. 1999. Multiple solenoidal microcoil probes for high-sensitivity, high-throughput nuclear magnetic resonance spectroscopy. *Anal. Chem.* 71:4815–20
54. Subramanian R, Webb AG. 1998. Design of solenoidal microcoils for high-resolution ^{13}C NMR spectroscopy. *Anal. Chem.* 70:2454–58
55. Subramanian R, Sweedler JV, Webb AG. 1999. Rapid two-dimensional inverse detected heteronuclear correlation experiments with <100 nmol samples with solenoidal microcoil NMR probes. *J. Am. Chem. Soc.* 121:2333–34
56. Kc R, Henry ID, Park GHJ, Raftery D. 2009. Design and construction of a versatile dual volume heteronuclear double resonance microcoil NMR probe. *J. Magn. Reson.* 197:186–92
57. Peck TL, Magin RL, Kruse J, Feng M. 1994. NMR microspectroscopy using 100 μm planar RF coils fabricated on gallium arsenide substrates. *IEEE Trans. Biomed. Eng.* 41:706–9
58. Stocker JE, Peck TL, Webb AG, Feng M, Magin RL. 1997. Nanoliter volume, high-resolution NMR microspectroscopy using a 60 μm planar microcoil. *IEEE Trans. Biomed. Eng.* 44:1122–27
59. Massin C, Boero G, Vincent F, Abenhaim J, Besse PA, Popovic RS. 2002. High–Q factor RF planar microcoils for micro-scale NMR spectroscopy. *Sens. Actuators A* 97/98:280–88
60. Massin C, Daridon A, Vincent F, Boero G, Besse PA, et al. 2001. *A microfabricated probe with integrated coils and channels for on-chip NMR spectroscopy*. Presented at Micro Total Anal. Syst. 2001, Monterey
61. Massin C, Vincent F, Homsy A, Ehrmann K, Boero G, et al. 2003. Planar microcoil–based microfluidic NMR probes. *J. Magn. Reson.* 164:242–55
62. Wensink H, Hermes DC, van den Berg A. 2004. *High signal to noise ratio in low field NMR on chip: simulations and experimental results*. Presented at Int. Workshop Micro Electromech. Syst., 7th, Maastricht, Neth.
63. Gomez MV, Reinhoudt DN, Velders AH. 2007. *Supramolecular chemistry in an NMR chip*. Presented at Micro Total Anal. Syst. 2007, Paris
64. Dolbier W. 2009. *Guide to Fluorine NMR for Organic Chemists*. New York: Wiley. 256 pp.
65. Gómez MV, Reinhoudt DN, Velders AH. 2008. Supramolecular interactions at the picomole level studied by ^{19}F NMR spectroscopy in a microfluidic chip. *Small* 4:1293–95
66. Leidich S, Braun M, Gessner T, Riemer T. 2009. Silicon cylinder spiral coil for nuclear magnetic resonance spectroscopy of nanoliter samples. *Concepts Magn. Reson. B* 35B:11–22
67. Anders J, Chiaramonte G, SanGiorgio P, Boero G. 2009. A single-chip array of NMR receivers. *J. Magn. Reson.* 201:239–49
68. Zhang X, Ugurbil K, Chen W. 2001. Microstrip RF surface coil design for extremely high-field MRI and spectroscopy. *Magn. Reson. Med.* 46:443–50
69. Maguire Y, Chuang IL, Zhang S, Gershenfeld N. 2007. Ultra-small-sample molecular structure detection using microslot waveguide nuclear spin resonance. *Proc. Natl. Acad. Sci. USA* 104:9198–203
70. Krojanski HG, Lambert J, Gerikalan Y, Suter D, Hergenröder R. 2008. Microslot NMR probe for metabolomics studies. *Anal. Chem.* 80:8668–72

71. van Bentum PJM, Janssen JWG, Kentgens APM. 2004. Towards nuclear magnetic resonance μ-spectroscopy and μ-imaging. *Analyst* 129:793–803
72. van Bentum PJM, Janssen JWG, Kentgens APM, Bart J, Gardeniers JGE. 2007. Stripline probes for nuclear magnetic resonance. *J. Magn. Reson.* 189:104–13
73. Bart J, Kolkman AJ, Oosthoek–de Vries AJ, Koch K, Nieuwland PJ, et al. 2009. A microfluidic high-resolution NMR flow probe. *J. Am. Chem. Soc.* 131:5014–15
74. Bart J, Janssen JWG, van Bentum PJM, Kentgens APM, Gardeniers JGE. 2009. Optimization of stripline-based microfluidic chips for high-resolution NMR. *J. Magn. Reson.* 201:175–85
75. Haswell SJ, Middleton RJ, O'Sullivan B, Skelton V, Watts P, Styring P. 2001. The application of micro reactors to synthetic chemistry. *Chem. Commun.* 2001:391–98
76. deMello AJ. 2006. Control and detection of chemical reactions in microfluidic systems. *Nature* 442:394–402
77. Dittrich PS, Tachikawa K, Manz A. 2006. Micro total analysis systems. Latest advancements and trends. *Anal. Chem.* 78:3887–908
78. West J, Becker M, Tombrink S, Manz A. 2008. Micro total analysis systems: latest achievements. *Anal. Chem.* 80:4403–19
79. Chiu DT, Lorenz RM, Jeffries GDM. 2009. Droplets for ultrasmall-volume analysis. *Anal. Chem.* 81:5111–18
80. Mir M, Homs A, Samitier J. 2009. Integrated electrochemical DNA biosensors for lab-on-a-chip devices. *Electrophoresis* 30:3386–97
81. Arora A, Simone G, Salieb-Beugelaar GB, Kim JT, Manz A. 2010. Latest developments in micro total analysis systems. *Anal. Chem.* 82:4830–47
82. Ríos A, Escarpa A, Simonet B. 2009. Detection in miniaturized analytical systems. In *Miniaturization of Analytical Systems: Principles, Designs, and Applications*, pp. 213–61. Chichester, UK: Wiley
83. Laude DA, Wilkins CL. 1984. Direct-linked analytical scale high-performance liquid chromatography/nuclear magnetic resonance spectrometry. *Anal. Chem.* 56:2471–75
84. Albert K. 1996. Hyphenation of chromatographic separation techniques with nuclear magnetic resonance spectroscopy: present status and future. *Analysis* 24:M17–18
85. Albert K. 1995. On-line use of NMR detection in separation chemistry. *J. Chromatogr. A* 703:123–47
86. Korhammer SA, Bernreuther A. 1996. Hyphenation of high-performance liquid chromatography (HPLC) and other chromatographic techniques (SFC, GPC, GC, CE) with nuclear magnetic resonance (NMR): a review. *Fresenius J. Anal. Chem.* 354:131–35
87. Lindon JC, Nicholson JK, Wilson ID. 1996. Direct coupling of chromatographic separations to NMR spectroscopy. *Prog. Nucl. Magn. Reson. Spectrosc.* 29:1–49
88. Albert K. 1997. Supercritical fluid chromatography–proton nuclear magnetic resonance spectroscopy coupling. *J. Chromatogr. A* 785:65–83
89. Albert K, Dachtler M, Glaser T, Händel H, Lacker T, et al. 1999. On-line coupling of separation techniques to NMR. *J. High Resolut. Chromatogr.* 22:135–43
90. Corcoran O, Spraul M. 2003. LC-NMR-MS in drug discovery. *Drug Discov. Today* 8:624–31
91. Webb AG. 2005. Nuclear magnetic resonance coupled microseparations. *Magn. Reson. Chem.* 43:688–96
92. Kühnle M, Holtin K, Albert K. 2009. Capillary NMR detection in separation science. *J. Sep. Sci.* 32:719–26
93. Wu N, Webb A, Peck TL, Sweedler JV. 1995. Online NMR detection of amino acids and peptides in microbore LC. *Anal. Chem.* 67:3101–7
94. Subramanian R, Kelley WP, Floyd PD, Tan ZJ, Webb AG, Sweedler JV. 1999. A microcoil NMR probe for coupling microscale HPLC with on-line NMR spectroscopy. *Anal. Chem.* 71:5335–39
95. Lacey ME, Tan ZJ, Webb AG, Sweedler JV. 2001. Union of capillary high-performance liquid chromatography and microcoil nuclear magnetic resonance spectroscopy applied to the separation and identification of terpenoids. *J. Chromatogr. A* 922:139–49
96. Albert K, Schlotterbeck G, Tseng L-H, Braumann U. 1996. Application of on-line capillary high-performance liquid chromatography–nuclear magnetic resonance spectrometry coupling for the analysis of vitamin A derivatives. *J. Chromatogr. A* 750:303–9

97. Behnke B, Schlotterbeck G, Tallarek U, Strohschein S, Tseng L-H, et al. 1996. Capillary HPLC–NMR coupling: high-resolution ^{1}H NMR spectroscopy in the nanoliter scale. *Anal. Chem.* 68:1110–15
98. Schlotterbeck G, Tseng L-H, Händel H, Braumann U, Albert K. 1997. Direct on-line coupling of capillary HPLC with ^{1}H NMR spectroscopy for the structural determination of retinyl acetate dimers:2D NMR spectroscopy in the nanoliter scale. *Anal. Chem.* 69:1421–25
99. Jorgenson JW, Lukacs KD. 1981. Zone electrophoresis in open-tubular glass capillaries. *Anal. Chem.* 53:1298–302
100. Ríos A, Escarpa A, Simonet B. 2009. Miniaturized systems for analytical separations. II: Systems based on electroosmotic flow. In *Miniaturization of Analytical Systems: Principles, Designs, and Applications*, pp. 165–211. Chichester, UK: Wiley
101. Olson DL, Lacey ME, Webb AG, Sweedler JV. 1999. Nanoliter-volume ^{1}H NMR detection using periodic stopped-flow capillary electrophoresis. *Anal. Chem.* 71:3070–76
102. Wolters AM, Jayawickrama DA, Webb AG, Sweedler JV. 2002. NMR detection with multiple solenoidal microcoils for continuous-flow capillary electrophoresis. *Anal. Chem.* 74:5550–55
103. Jayawickrama DA, Sweedler JV. 2004. Dual microcoil NMR probe coupled to cyclic CE for continuous separation and analyte isolation. *Anal. Chem.* 76:4894–900
104. Kautz RA, Lacey ME, Wolters AM, Foret F, Webb AG, et al. 2001. Sample concentration and separation for nanoliter-volume NMR spectroscopy using capillary isotachophoresis. *J. Am. Chem. Soc.* 123:3159–60
105. Wolters AM, Jayawickrama DA, Larive CK, Sweedler JV. 2002. Capillary isotachophoresis/NMR: extension to trace impurity analysis and improved instrumental coupling. *Anal. Chem.* 74:2306–13
106. Jayawickrama D, Sweedler J. 2004. Chiral separation of nanomole amounts of alprenolol with cITP/NMR. *Anal. Bioanal. Chem.* 378:1528–35
107. Almeida VK, Larive CK. 2005. Insights into cyclodextrin interactions during sample stacking using capillary isotachophoresis with on-line microcoil NMR detection. *Magn. Reson. Chem.* 43:755–61
108. Pusecker K, Schewitz J, Gfrörer P, Tseng L-H, Albert K, Bayer E. 1998. On-line coupling of capillary electrochromatography, capillary electrophoresis, and capillary HPLC with nuclear magnetic resonance spectroscopy. *Anal. Chem.* 70:3280–85
109. Pusecker K, Schewitz J, Gfrorer P, Tseng L-H, Albert K, et al. 1998. On-flow identification of metabolites of paracetamol from human urine by using directly coupled CZE-NMR and CEC-NMR spectroscopy. *Anal. Commun.* 35:213–15
110. Trumbull JD, Glasgow IK, Beebe DJ, Magin RL. 2000. Integrating microfabricated fluidic systems and NMR spectroscopy. *IEEE Trans. Biomed. Eng.* 47:3–7
111. Geyer K, Codée JDC, Seeberger PH. 2006. Microreactors as tools for synthetic chemists—the chemists' round-bottomed flask of the 21st century? *Chem. A Eur. J.* 12:8434–42
112. Kakuta M, Jayawickrama DA, Wolters AM, Manz A, Sweedler JV. 2003. Micromixer-based time-resolved NMR: applications to ubiquitin protein conformation. *Anal. Chem.* 75:956–60
113. Ciobanu L, Jayawickrama DA, Zhang X, Webb AG, Sweedler JD. 2003. Measuring reaction kinetics by using multiple microcoil NMR spectroscopy. *Angew. Chem. Int. Ed.* 42:4669–72
114. Gomez MV, Verputten HHJ, Diaz-Ortiz A, Moreno A, de la Hoz A, Velders AH. 2010. On-line monitoring of a microwave-assisted chemical reaction by nanolitre NMR-spectroscopy. *Chem. Commun.* 46:4514–16
115. Wensink H, Benito-Lopez F, Hermes DC, Verboom W, Gardeniers JGE, et al. 2005. Measuring reaction kinetics in a lab-on-a-chip by microcoil NMR. *Lab Chip* 5:280–84
116. McDowell AF, Adolphi NL. 2007. Operating nanoliter scale NMR microcoils in a 1 tesla field. *J. Magn. Reson.* 188:74–82
117. Wright AC, Neideen TA, Magin RL, Norcross JA. 1998. Evaluation of radio frequency microcoils as nuclear magnetic resonance detectors in low-homogeneity high-field superconducting magnets. *Rev. Sci. Instrum.* 69:3938–41

RELATED RESOURCES

1. **http://www.bruker-biospin.com**
2. **http://www.chem.agilent.com**
3. **http://www.jeol.com**
4. **http://www.protasis.com/MicroFlowNMR/index.htm**

Annual Review of
Analytical Chemistry

Volume 4, 2011

Contents

A Century of Progress in Molecular Mass Spectrometry
Fred W. McLafferty 1

Modeling the Structure and Composition of Nanoparticles by Extended X-Ray Absorption Fine-Structure Spectroscopy
Anatoly I. Frenkel, Aaron Yevick, Chana Cooper, and Relja Vasic 23

Adsorption Microcalorimetry: Recent Advances in Instrumentation and Application
Matthew C. Crowe and Charles T. Campbell 41

Microfluidics Using Spatially Defined Arrays of Droplets in One, Two, and Three Dimensions
Rebecca R. Pompano, Weishan Liu, Wenbin Du, and Rustem F. Ismagilov 59

Soft Landing of Complex Molecules on Surfaces
Grant E. Johnson, Qichi Hu, and Julia Laskin 83

Metal Ion Sensors Based on DNAzymes and Related DNA Molecules
Xiao-Bing Zhang, Rong-Mei Kong, and Yi Lu 105

Shell-Isolated Nanoparticle-Enhanced Raman Spectroscopy: Expanding the Versatility of Surface-Enhanced Raman Scattering
Jason R. Anema, Jian-Feng Li, Zhi-Lin Yang, Bin Ren, and Zhong-Qun Tian 129

High-Throughput Biosensors for Multiplexed Food-Borne Pathogen Detection
Andrew G. Gehring and Shu-I Tu 151

Analytical Chemistry in Molecular Electronics
Adam Johan Bergren and Richard L. McCreery 173

Monolithic Phases for Ion Chromatography
Anna Nordborg, Emily F. Hilder, and Paul R. Haddad 197

Small-Volume Nuclear Magnetic Resonance Spectroscopy
Raluca M. Fratila and Aldrik H. Velders 227

The Use of Magnetic Nanoparticles in Analytical Chemistry
Jacob S. Beveridge, Jason R. Stephens, and Mary Elizabeth Williams 251

Controlling Mass Transport in Microfluidic Devices
Jason S. Kuo and Daniel T. Chiu 275

Bioluminescence and Its Impact on Bioanalysis
Daniel Scott, Emre Dikici, Mark Ensor, and Sylvia Daunert 297

Transport and Sensing in Nanofluidic Devices
Kaimeng Zhou, John M. Perry, and Stephen C. Jacobson 321

Vibrational Spectroscopy of Biomembranes
Zachary D. Schultz and Ira W. Levin 343

New Technologies for Glycomic Analysis: Toward a Systematic Understanding of the Glycome
John F. Rakus and Lara K. Mahal 367

The Asphaltenes
Oliver C. Mullins 393

Second-Order Nonlinear Optical Imaging of Chiral Crystals
David J. Kissick, Debbie Wanapun, and Garth J. Simpson 419

Heparin Characterization: Challenges and Solutions
Christopher J. Jones, Szabolcs Beni, John F.K. Limtiaco, Derek J. Langeslay, and Cynthia K. Larive 439

Indexes

Cumulative Index of Contributing Authors, Volumes 1–4 467

Cumulative Index of Chapter Titles, Volumes 1–4 470

Errata

An online log of corrections to the *Annual Review of Analytical Chemistry* articles may be found at http://arjournals.annualreviews.org/errata/anchem